International Journal of Mass Spectrometry 309 (2012) 148–153

Contents lists available at SciVerse ScienceDirect

International Journal of Mass Spectrometry

journal homepage: www.elsevier.com/locate/ijms

Quasi-non-destructive isotopic ratio measurement of boron in irradiated control rod B_4C pellets using a home-built reflectron time-of-flight mass spectrometer

P. Manoravi, M. Joseph*, N. Sivakumar, P.R. Vasudeva Rao

Chemistry Group, Indira Gandhi Centre for Atomic Research, Kalpakkam – 603 102, India

ARTICLE INFO

Article history:
Received 3 July 2011
Received in revised form
15 September 2011
Accepted 15 September 2011
Available online 1 October 2011

Keywords:
Laser mass spectrometry
Boron carbide

ABSTRACT

An experimental facility has been built for the analysis of the isotopic ratio $^{10}B/^{11}B$ in the stacked boron carbide (B_4C) pellets used as control rod in the Fast Breeder Test Reactor (FBTR). Measurements were made on 5 pellets. The values obtained for a control rod removed after the reactor core had seen a peak burn-up of ~100 GWd/t indicated a consumption of less than 1% of ^{10}B.

1. Introduction

Boron carbide (B_4C) is widely used as control rod material both in thermal reactors such as pressurized water reactors (PWR) and in fast breeder reactors (FBR). The absorption cross-sections of ^{10}B and ^{11}B for thermal neutrons are 3837 b and 5 mb, respectively, while the values for fast neutrons (~100 keV) are about 2.7 b for ^{10}B and a much smaller value (9.7×10^{-5} b) for ^{11}B [1]. The natural abundance of isotopes of boron are: 19.89% of ^{10}B and 80.11% of ^{11}B [2]. Hence, B_4C pellets enriched in ^{10}B are used in the control rods for FBRs. The extent of enrichment varies from 60%, for a commercial fast reactor, to as high as 90% for small core test reactors, such as our Fast Breeder Test Reactor (FBTR) [3]. Typically, the B_4C pellets used in the control rods of fast reactors are ≈10–40 mm in diameter and up to 50 mm in length. The pellets used in the control rod for FBTR are 38 mm in diameter and 40 mm in length. The density is 2.25 g/cc.

The consumption of ^{10}B present in B_4C pellets of a control rod is normally small as the rod is positioned out side of the active core level for a considerable part of its life in a reactor and the maximum burn-up of ^{10}B occurs only in the lower part of the pin. The life of a control rod is determined rather by the stability of the stainless steel clad in the radioactive environment. But to decide if the pellets from such an irradiated pin can be reused or be relocated (provided it has not suffered considerable change in isotopic ratio, dimensions or integrity), one needs to assured of sufficient abundance of ^{10}B in that pellets. The measurements of the abundance of ^{10}B required to be accurate to within ±1%. Though neutron irradiated B_4C is not expected to be radioactive, the common trace impurities present in the B_4C pellet can through neutron activation lead to considerable accumulation of radioactive isotopes [4]. Results of neutron activation analysis of a typical B_4C sample indicated the presence of following radioactive isotopes, namely, ^{152}Eu, ^{154}Eu, ^{182}Ta, ^{60}Co and ^{137}Cs arising from impurities [5]. Hence, it is important to have a suitable shielded enclosure (for β and γ activity) for the analysis of irradiated B_4C pellets if sufficient cooling period is not provided. Therefore, the method used for the $^{10}B/^{11}B$ ratio measurements on irradiated B_4C pellets needs to be amenable to remote operation.

Any destructive method for analysis of the isotope ratio of B in B_4C is cumbersome, as B_4C is one of the hardest materials known, next only to diamond and cubic boron nitride. Hence, a non-destructive method is preferred, not only to avoid the difficult dissolution or powdering process, but also because the pellet taken for analysis can be reused as it is, after the measurement.

Isotopic analysis of B is required in many fields of research and technology. The accuracy and precision to which isotopic composition is required depends on the nature of application. For instance in sub-nanogram sized foraminifera samples, one needs to measure very small variation (−50‰ to +50‰) compared to natural isotopic composition [6,7]. Whereas, in the boron enrichment plant (20–90 atom%), the accuracy needed is about ±1 atom% [8]. Hence, depending on the demand, a variety of methods, such as TIMS [7,9], ICPMS [7,10], SIMS [11] and ES–MS [12], are employed. However, laser ionization mass spectrometry (LIMS) is a suitable method, for the present application, amenable to remote operation and practically non-destructive. In LIMS, a focused laser beam generates ions

* Corresponding author. Tel.: +91 44 27480098; fax: +91 44 27480065.
E-mail address: mj@igcar.gov.in (M. Joseph).

1387-3806/$ – see front matter © 2011 Elsevier B.V. All rights reserved.
doi:10.1016/j.ijms.2011.09.012

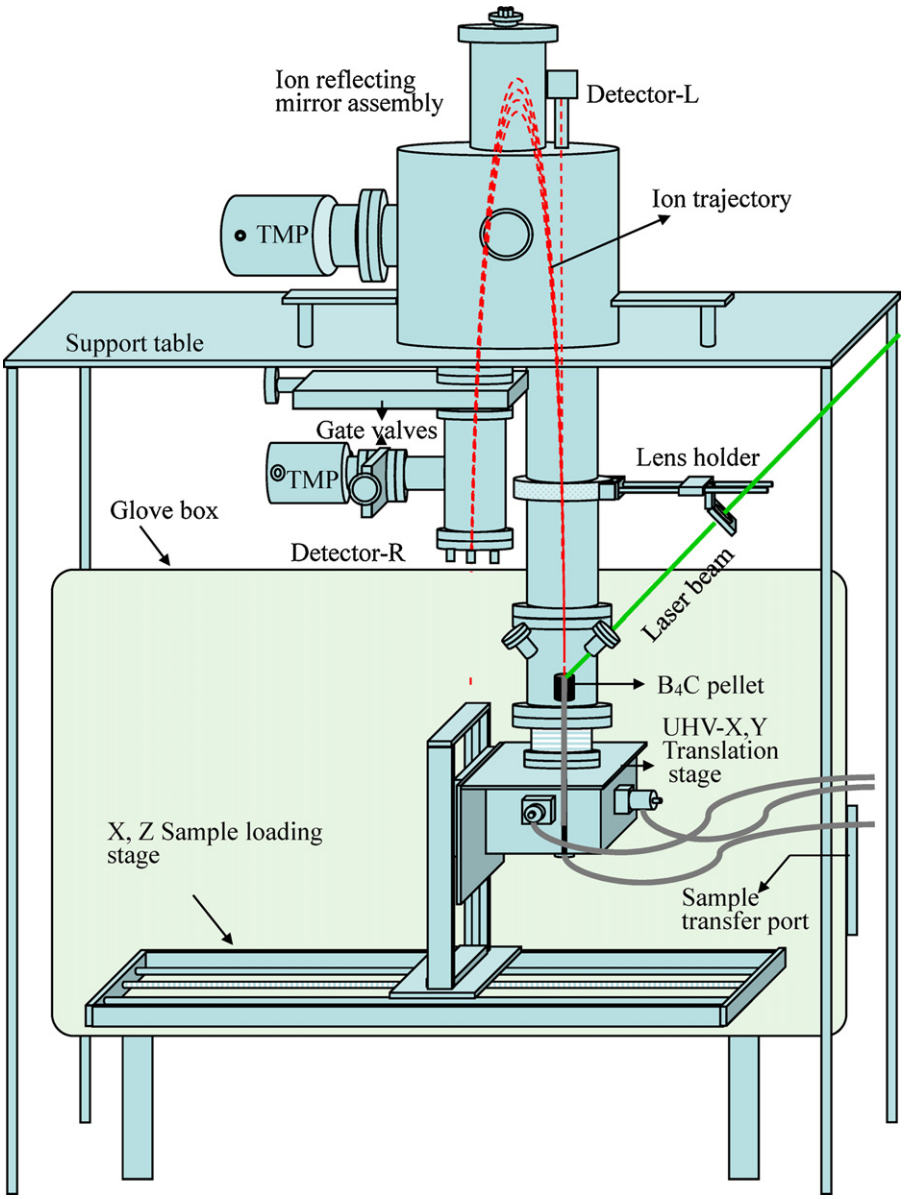

Fig. 1. Schematic diagram of home-built reflectron time-of-flight mass spectrometer for the analysis of $^{10}B/^{11}B$ ratio in FBTR control rod B_4C pellets [8].

from a very small area (~2 mm–100 μm in diameter and the power density used ranges from 10^6 to 10^{10} W/cm^2) on the sample surface through vaporization–ionization and the ions are mass analyzed. In many studies a time-of-flight mass spectrometer (TOFMS) is used for mass analysis. For a 10 ns wide laser pulse used, the vaporization removes only a few nanograms of the material from the focal area on the surface. There is no physical damage to the pellet (for a nanosecond laser pulse used, the transiently heated layer is expected to be only a few tens or hundreds of Å depth [13]). Therefore LIMS serves as a non-destructive analytical method. Generally in LIMS, where laser ablation/ionization is coupled to TOFMS for the analysis of solid samples, quantification is based on their absolute intensities of the ionic species by adopting one of the following methods: (i) use a post-ionization method (such as inductively coupled plasma or resonance ionization); (ii) incorporate a very narrow energy window with a very large acceleration energy, of the order of 10–20 keV (to suppress the energy spread arising from the ion formation process; further more one need to have matrix matched standards and suitable laser beam) [14]. However, arrangements of such techniques (i & ii) increase the complexity of the instrument, whereas the instrumentation used in the present work is very simple, which permits determination of ^{10}B isotope abundance by measuring the ion intensity ratios of $^{10}B^+/^{11}B^+$. The home-built reflectron time-of-flight mass spectrometer (TOFMS) is of Mamyrin type [15]. In this paper, we describe briefly this facility and the results of measurements of the isotope ratio $^{10}B/^{11}B$ in the irradiated B_4C pellets of a control rod removed from FBTR.

2. Experimental

A schematic diagram of LIMS facility is given in Fig. 1 and the details of various components used, are discussed elsewhere [8]. Briefly, the facility consists of five parts: (i) bellow assembly with the sample holder on a X, Y translation stage; (ii) sample chamber; (iii) drift tube; (iv) ion mirror; and (v) detector chamber. The bellow assembly and the sample chamber are housed inside a glove box and the remaining are kept outside. The drift tube of the TOFMS runs vertically through the glove box, with a O-ring seal to the box through a flange integrated to the drift tube using a bellow for flexibility. The whole system, other than the detector chamber

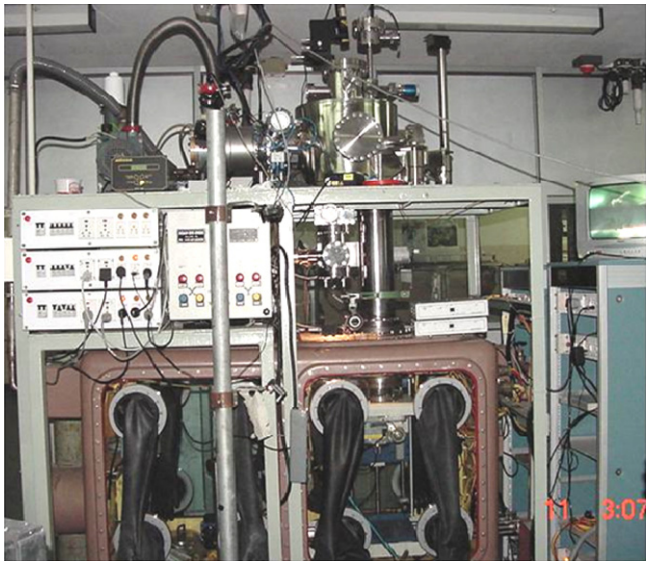

Fig. 2. Photograph of the reflectron TOFMS assembly along with glove box.

is pumped by a turbo molecular pump (TMP) having a pumping speed of 450 L/s and the detector chamber is pumped additionally by another TMP of 80 L/s capacity. The typical vacuum attained (without baking) during experiments is $\sim 3 \times 10^{-7}$ mbar.

The sample chamber has many user ports and view ports. The sample position is viewed remotely using small CCD cameras kept at two of the view ports of this chamber. The laser beam is focussed on the sample through a third view port. This chamber also holds two deflection plates for optimizing the angle of the ion trajectory in to the ion mirror. An electrical feed-through attached to this chamber is used to apply the voltages to these deflection plates and to the sample (through the sample holder).

In the bellow assembly for the positioning the sample, the sample holder is mounted on a stainless steel rod of 10 mm diameter which in turn mounted on a X, Y translation stage (UHV compatible). Scanning of the sample surface is done using this stage and the movement is remotely controlled by two DC motors. This stage does not have encoders to indicate the exact position of the stage during the operation but has limit switches. For each sample nearly ten points are taken across the 38 mm sample diameter by visual positioning of the laser focal spot (approximately evenly spaced). The laser spot size is ~2 mm. The bellow assembly with the X, Y stage is mounted on another X, Z translation stage provided on the floor of the glove box and its motion is controlled by two AC motors. This remotely controlled X, Z stage provides easy and quick loading/unloading of the radioactive samples. In the sample holder, sample (B_4C pellet of FBTR control rod) is placed in a cup made of stainless steel isolated electrically by placing the sample cup in a polytetrafluoroethylene (PTFE) cup. Fig. 2 shows the photograph of the overall experimental facility.

The second harmonic (532 nm) of a Q-switched Nd-YAG laser, with a pulse width of 8 ns and a repetition rate of 10 Hz is used. The pulse energy used was optimized to a value of 0.8–1 mJ/pulse and the corresponding power density for the focussed beam was of the order of 10^6 W/cm^2 [8]. A quartz lens with a focal length of 50 cm was used for focussing the laser beam and the target was positioned after the focus. The focal area used was large (2 mm dia). Use of larger power density results a large spread in the kinetic energy of the ions degrading the mass resolution [16].

A secondary electron multiplier (SEM) having a sensitive area of ~10 mm × 25 mm, rise time of ~2.0 ns, and recovery time of <5 ns is used as the detector. The typical gain of the detector is $\sim 1 \times 10^6$ at 2.8 kV, the optimized operating voltage in these measurements.

Table 1
Experimental parameters.

Mass resolution	300 (m/Δm)
Acceleration voltage	930 V
Detector voltage	−2.8 kV
TOFMS background pressure	3×10^{-7} mbar
Laser wavelength	Nd:YAG, 532 nm
Laser pulse energy	~1.0 mJ
Pulse duration	8 ns
Beam profile	TEM_{00} mode
Repetition rate	10 Hz
Laser spot size	2 mm dia.
Laser power density	3×10^6 W/cm^2

The bare SEM detector provided by the supplier was mounted on a 6″ OD CF flange with the required electrical connectors for the high voltage and signal leads. The signal from the SEM amplified and then recorded using a fast digital storage oscilloscope (DSO), interfaced to a PC through a GPIB (general purpose interface bus) for data collection. The DSO is triggered externally by a fast photodiode illuminated by a diffusive reflection of the laser beam. Hence, each laser pulse yields one sweep. Each spectrum is obtained for 1000 sweeps, and summation average mode (available in the DSO) is used to improve the signal to noise. All the experimental parameters are summarized in Table 1.

A stack of nine B_4C pellets (38 mm dia and 40 mm length), 90% enriched in ^{10}B and contained in a stainless steel clad, is used as control rod in our FBTR) [17]. The control rod had seen an effective full power day operation of 653 days since the criticality of FBTR before it was discharged from the core. At the time of discharge of the control rod, the core had a peak burn-up of 102 GWd/t. After cutting open the clad of the control rod in a hot cell, the irradiated pellets were taken out and cleaned using alcohol in order to remove the sodium, the coolant. Out of the nine pellets, five pellets namely 1st, 3rd, 6th, 8th and 9th pellets (9th being the bottom most pellet) were analyzed for the $^{10}B/^{11}B$ isotopic ratio. These pellets were loaded in the LIMS without any further sample processing.

Except pellets 1 and 3, others were received as non-cylindrical, irregular broken pieces. The pellets may have been broken during their removal from the control rod clad. It is known that the B_4C pellets loose their integrity above a burn-up of 5% of ^{10}B [18] and this is another possible reason. In order to analyze the irregular shaped B_4C solid pieces, graphite holders were made with appropriate cavity matching the shape of the sample pieces, approximately. Such an arrangement was found necessary to keep the electrical field uniformity at the acceleration region in the sample holder of the mass spectrometer.

3. Results and discussion

Initial experiments for standardizing the method were done using unirradiated B_4C samples. For the measurement of the $^{10}B/^{11}B$ ratio in B_4C using the LIMS method, one needs to have sufficient number of B ions be formed during the laser heating while the laser power density is sufficiently small that no large spread in the translational energy distribution of ions occurs which will degrade the mass resolution. The expansion of the plume must not introduce any mass dependence in the sampling [19]. In the present experiments, the optimum laser power density employed is $\sim 3 \times 10^6$ W/cm^2 [8].

A typical time-of-flight mass spectrum obtained for irradiated and unirradiated B_4C pellets are shown in Fig. 3(a) and the expanded isotope peaks of boron are shown in Fig. 3(b). Even though the flight time (Fig. 3(a)) shown here is only up to 60 μs (corresponding to 120 amu), the spectrum was collected for 200 μs (up to 600 amu), and it did not show the presence of any other species. Earlier, Becker and Dietze, have studied B_4C using LIMS

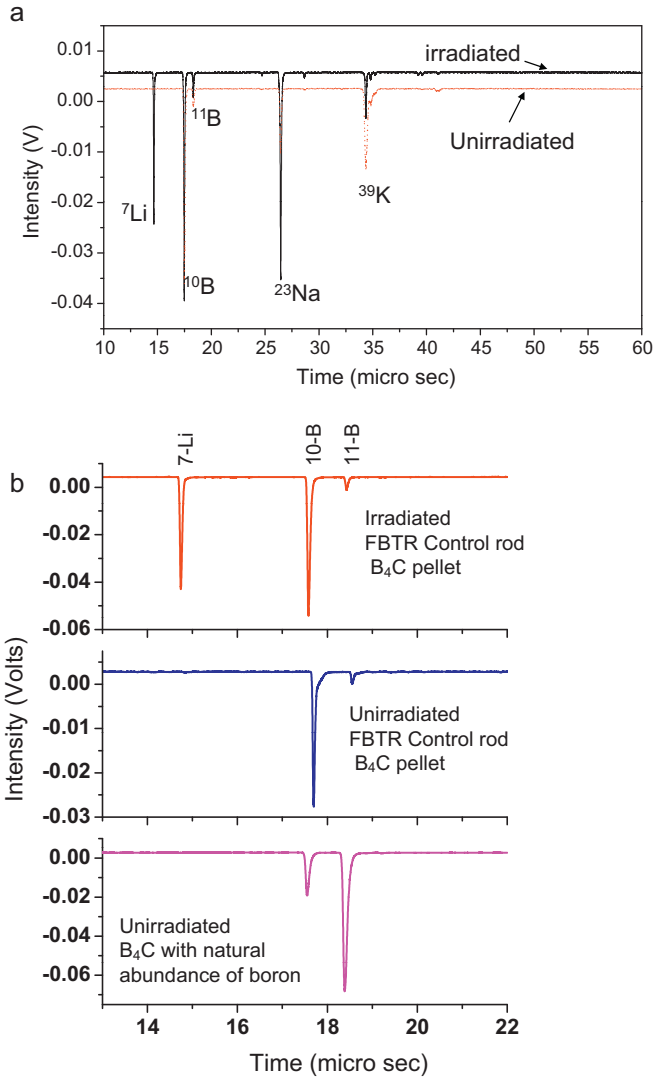

Fig. 3. (a) Typical mass spectra obtained for irradiated and unirradiated B_4C pellets; (b) expanded view of the above mass spectra, including that of natural abundance B_4C pellet.

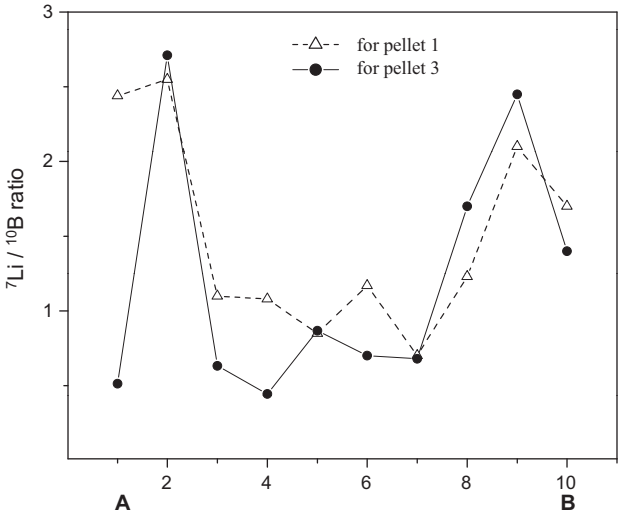

Fig. 4. ^{7}Li/^{10}B for different spatial locations on the 1st and 3rd pellets.

and observed cluster ions of the type B_nC_m $(n+m=17)$ [20]. In their study, the parameters of the Nd-YAG laser used is very different from the one used in the present study (see Table 1); they have used a pulse width of 100 ns, the fundamental wave length (1064 nm), very high reparation rate of 10 kHz and high power density (5×10^8 W/cm^2). With these laser parameters, the vaporization/ionization process can be very different. Higher the vaporization temperature, larger the vapor pressure and more clusterisation is expected. Larger temperature can give rise to more complex vapor species [21]; a possible reason for the observation of higher mass species in their study. As can be seen from Fig. 3(a), sodium and potassium peaks are observed in both natural and irradiated pellets. These peaks are due to contamination. Source of Na and K impurities in the case of unirradiated sample is the bare-hand handling of the pellets. Irradiated B_4C pellets are in contact with liquid sodium (the coolant) as the control rod pins are of vented type (to facilitate removal of He gas produced due to neutron absorption by ^{10}B) one would expect traces of sodium (with potassium as impurity) though the sodium is removed by alcoholic wash. As can be seen from Fig. 3(b), there is an appreciable intensity of ^{7}Li, but there is no trace of ^{6}Li. If the observed ^{7}Li were to be from natural contamination, we should have observed ^{6}Li also whose natural abundance is 7.5% [2]. Therefore, we infer that presence of ^{7}Li is due to the processes of consumption of ^{10}B through the (n,α) reaction: $^{10}B + {}^{1}n \rightarrow {}^{4}He + {}^{7}Li$. For a fast reactor core, $^{10}B(n,2\alpha)^{3}H$ reaction is also possible, thereby producing tritium in addition to helium in the B_4C matrix [22]. It is likely that tritium and helium ion densities are negligible in the vapor for the laser intensity used in these studies because of their larger ionization potentials and hence are not detected.

As can be seen from the above figure, the ion signals for $^{10}B^+$ and $^{11}B^+$ ions are well resolved, with a time difference of ≈0.9 μs for an ion flight energy of 930 eV. For pellets 1 and 3, measurements were done across the diameter on both faces of the cylindrical pellet. Results indicated no definite variation in the abundance of ^{10}B. The ^{10}B percentage was deduced from the ratio of the areas under the peaks corresponding to the isotopes of ^{10}B and ^{11}B for a given laser pulse (vaporization and ionization in one single step). A typical result obtained for measurement of percentage of ^{10}B in 1st pellet is shown in Table 2. Earlier study [8] indicated that in order to get good signal to noise ratio, it is necessary to sum average for at least 500 sweeps. At each laser spot, a set of five mass spectra are recorded, each spectrum a sum average of 1000 sweeps. Measurements are done at 10 spots, approximately evenly spaced, across the 38 mm diameter of the pellet.

It was possible to examine the radial profile of ^{10}B abundance only in the 1st and the 3rd pellets as these were received in regular shape. While our ^{10}B abundance measurements did not show any systematic change with position, we could observe some indicative correlation from the ^{7}Li to ^{10}B ratio for different radial locations of laser focal area. As shown in Fig. 4, close to the periphery of the pellet (A and B in the figure), the ^{7}Li/^{10}B ratios are larger – indicating higher burn-up of ^{10}B in the periphery.

SIMS analysis of irradiated boron carbide samples has been reported in the literature [22]. These were hot isostatically pressed boron carbide pellets of 1.75 mm dia and 10 mm long, irradiated for 2 years in a light water nuclear power reactor (PWR). This study indicated a larger burn-up of ^{10}B close to the periphery of the pellet compared to the centre. But a flat profile was reported for Li (non-specific on the isotopic nature) as a function of sample position on the pellet. It was concluded that the Li observed was due to contamination of the sample during its preparation in a wet environment. In another study, with the objective of determination of Li diffusion coefficient, B_4C pellets (6.6 mm dia and 11 mm long) were irradiated in FBR (Phenix) for two months and then the pellet was cut into 1 mm thick discs, annealed and Li concentration was measured

Table 2
The ratios of $^{10}B/^{11}B$ measured in terms of area under the peak and the enrichment obtained for a typical experiment performed on the 1st pellet of the control rod. Measurements are done at 10 spots (approximately evenly spaced and the spot dia is about 2 mm) across the 38 mm dia, B_4C pellet. A correction factor 0.997 is applied by comparing the % of enrichment obtained for unirradiated B_4C pellet using present LMS and TIMS values [9].

Spot number on B_4C pellet	Area of ^{10}B peak (A_{10}) (a.u.)	Area of ^{11}B peak (A_{11}) (a.u.)	Ratio (A_{10}/A_{11})	% of ^{10}B in B_4C[a]	Average of % of ^{10}B
1	1.81E-3	1.742E-4	10.39	90.95	
	1.85E-3	1.787E-4	10.35	90.92	
	1.38E-3	1.387E-4	9.95	90.59	
	1.4E-3	1.448E-4	9.67	90.36	
	1.14E-3	1.166E-4	9.78	90.45	90.7 ± 0.3
2	8.523E-4	8.438E-5	10.10	90.72	
	6.715E-4	6.79E-5	9.89	90.54	
	4.894E-4	5.015E-5	9.76	90.43	
	4.039E-4	4.143E-5	9.75	90.43	
	1.824E-4	1.859E-5	9.81	90.48	90.5 ± 0.1
3	1.34E-3	1.311E-4	10.22	90.82	
	7.895E-4	7.565E-5	10.44	90.98	
	6.636E-4	6.458E-5	10.28	90.86	
	5.022E-4	5.172E-5	9.71	90.39	
	3.73E-4	3.803E-5	9.81	90.47	90.7 ± 0.3
4	1.21E-3	1.226E-4	9.87	90.53	
	1E-3	1.007E-4	9.93	90.58	
	7.656E-4	7.77E-5	9.85	90.51	
	4.115E-4	4.115E-5	10.00	90.64	
	4.977E-4	5.195E-5	9.58	90.28	90.5 ± 0.2
5	9.243E-4	8.903E-5	10.38	90.94	
	7.189E-4	7.211E-5	9.97	90.61	
	5.314E-4	5.498E-5	9.67	90.35	
	7.984E-4	7.772E-5	10.27	90.86	
	5.227E-4	5.437E-5	9.61	90.31	90.6 ± 0.3
6	2.07E-3	2.029E-4	10.20	90.80	
	1.61E-3	1.592E-4	10.11	90.73	
	1.08E-3	1.131E-4	9.55	90.25	
	1.16E-3	1.203E-4	9.64	90.33	
	9.89E-4	1.03E-4	9.60	90.29	90.5 ± 0.3
7	5.4E-4	5.439E-5	9.93	90.58	
	8.843E-4	8.782E-5	10.07	90.69	
	6.724E-4	7.084E-5	9.49	90.20	
	5.418E-4	5.433E-5	9.97	90.61	
	4.726E-4	4.647E-5	10.17	90.77	90.6 ± 0.2
8	2.44E-3	2.442E-4	9.99	90.63	
	2.6E-3	2.633E-4	9.87	90.53	
	2.36E-3	2.413E-4	9.78	90.45	
	4.015E-4	4.035E-5	9.95	90.60	
	2.796E-4	2.82E-5	9.91	90.57	90.6 ± 0.1
9	2.08E-3	2.027E-4	10.26	90.85	
	2.04E-3	2.142E-4	9.52	90.23	
	1.49E-3	1.557E-4	9.57	90.26	
	1.35E-3	1.435E-4	9.41	90.12	
	1.15E-3	1.178E-4	9.76	90.44	90.4 ± 0.3
10	2.891E-4	3.041E-5	9.51	90.21	
	9.656E-4	1.007E-4	9.59	90.28	
	8.545E-4	8.258E-5	10.35	90.91	
	8.435E-4	8.769E-5	9.62	90.31	
	7.23E-4	7.459E-5	9.69	90.38	90.4 ± 0.3

[a] % of ^{10}B in $B_4C = (A_{10}/A_{11})/(1 + (A_{10}/A_{11})) \times 100 \times 0.997$.

using a nuclear microprobe technique [23]. Quantitative measurement of ^7Li concentration cannot be performed in our study because the ionization potential of Li and B are very different, and therefore ion density in the vapor for Li and B will be different by orders of magnitude for the same temperature of the transiently heated sample surface. Literature indicates that quantitative measurement of most elements is possible with laser ablation/ionization, using a high laser power density (10^9–10^{10} W/cm^2 using short duration pulses – ps or less, and wavelength in UV region) with a suitable mass analyzer and calibration standards [24,25]. At such high laser power densities it is possible to get almost unit ionization probability for most of the elements. However, in our system we cannot use laser power densities higher than 10^7 W/cm^2, because of loss of mass resolution [16] and the possibility of isotope enrichment in different parts of the plume in the expansion when the power density is above 2×10^8 W/cm^2 [19]. Further more, the main objective of the present work is to determine the percentage of ^{10}B present in these irradiated control rod pellets and not determination of different elements. As the present method involves measurement of the intensity ratio of the isotopes of the same element, namely boron, any pulse to pulse energy variation of the laser system will not cause any bias.

The measured percentages of ^{10}B as a function of spot position for various pellets are shown in Fig. 5 including that of 1st pellet, for which the numerical values are given in Table 2. Results from all the pellets analyzed show that there is no significant consumption of ^{10}B (<1%). This result implies that the likely possible reason for the fracture of the pellets removed is the stress during the removal from the clad. The average value of % of ^{10}B measured along with the theoretically calculated values [26] is shown in Fig. 6. The measured depletion of % of ^{10}B is less than the calculated values. The calculation of burn-up of ^{10}B is done in a very conservative way. In this calculation, the value of the neutron flux used corresponds to a situation where the control rods are completely out of the core (peak

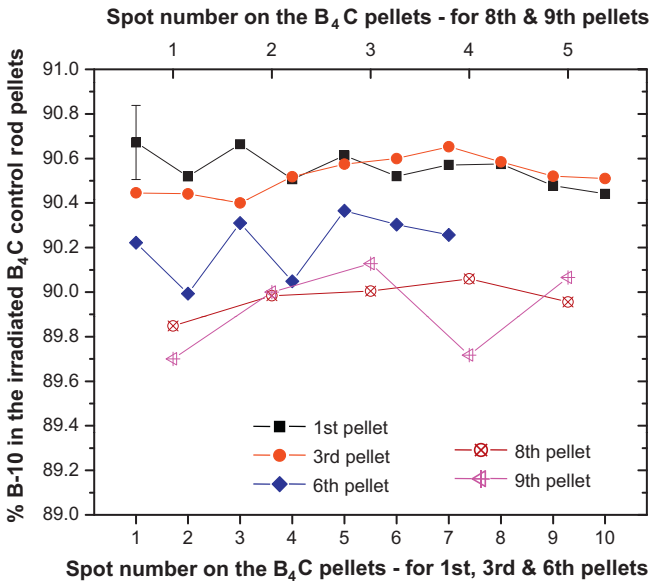

Fig. 5. % ^{10}B for different spatial locations on the irradiated pellets (numerical data for 1st pellet is shown in Table 2).

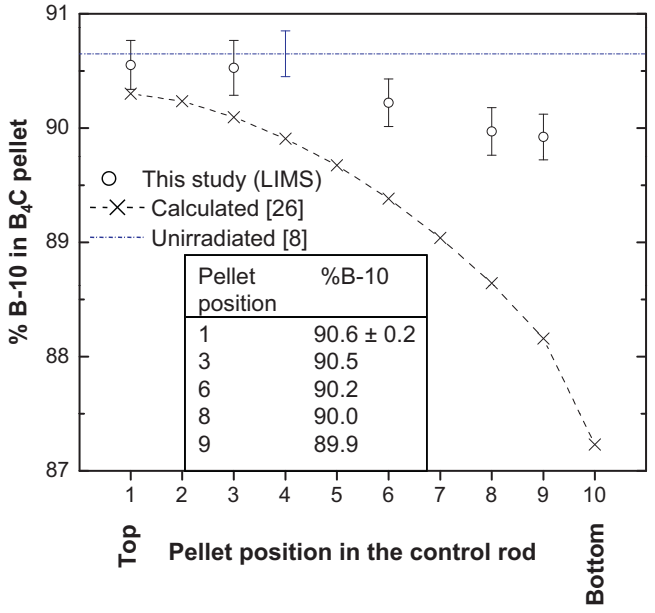

Fig. 6. Measured % ^{10}B in comparison with calculated values [26] (insert indicates the measured values).

flux). For the calculation of burn-up of ^{10}B, control rod is assumed to be at the centre of the core and kept in half-way position. Since control rod is continuously withdrawn as the reactor operates, the control rod moves from higher flux to lower flux region. Hence the calculated burn-up are expected to be on the higher side, compared to the actual burn-up. In this calculation, only (n,α) is considered as the depletion mechanism. It is to be noted that (n,α) cross section is very high for thermal neutrons compared to the neutron spectrum for FBTR, which has a very small thermal neutron flux component. Large percentage error in thermal flux will not affect major reactor physics calculations like K_{eff} and power distribution, but can affect (n,α) reactions in ^{10}B. Hence, even a relatively small error in the component of thermal flux can lead to large errors in the calculated ^{10}B depletion.

4. Conclusions

An in-house developed LIMS facility is used to measure isotopic ratio ^{10}B/^{11}B in the irradiated B_4C pellets of the FBTR control rod. This laser-based technique for B isotope ratio measurements is advantageous compared to the conventional mass spectrometric methods in terms of being practically non-destructive, fast, less expensive, and easy to adapt for remote operation. Measurements of % of ^{10}B were done on 5 pellets. The values % of ^{10}B obtained indicated very small (less than 1%) consumption of ^{10}B. The observed ratio of ^{7}Li/^{10}B indicates a larger concentration of ^{7}Li in the periphery compared to the centre of the pellet.

Acknowledgements

The authors are grateful to Dr. R. Viswanathan, Head, Mass Spectrometric Studies Section and Dr. C.P. Reddy, Head, Reactor Physics Section for useful discussions.

References

[1] A.G. Rafi Ahmed, Sujoy Sen, V. Goplalakrishnan, Cross-sections of some control-rod materials for PFBR, Report No. RPD/NDS/103, Indira Gandhi Centre for Atomic Research, January 2003.
[2] Hand Book of Chemistry and Physics, 73rd ed., CRC press, 1992–1993, pp. 11–28.
[3] S.C. Chetal, V. Balasubramaniyan, P. Chellapandi, P. Mohanakrishnan, P. Puthiyavinayagam, C.P. Pillai, S. Raghupathy, T.K. Shanmugham, C. Sivathanu Pillai, Nucl. Eng. Des. 236 (2006) 852.
[4] V.D. Risovany, A.V. Zakharov, E.P. Klochkov, A.G. Osipenko, N.S. Kosulin, G.I. Mikhailichenko, Proceeding of a Technical Committee meeting on 'Absorber materials, control rods and designs of shutdown systems for advanced liquid metal fast reactors' IAEA-TECDOC-884, 1996, pp. 219–224.
[5] P.R. Vasudeva Rao, S. Anthonysamy, Characterization of B4C Control Rod Sample, IGC:FChD, 2003, pp. 221–214 (dt. 8/July/2003).
[6] G.L. Foster, Y. Ni, B. Haley, T. Elliott, Chem. Geol. 230 (2006) 161.
[7] S.A. Kasemann, D.N. Schmidt, J. Bijma, G.L. Foster, Chem. Geol. 260 (2009) 138.
[8] P. Manoravi, M. Joseph, N. Sivakumar, Int. J. Mass Spectrom. 276 (2008) 9.
[9] B. Chetelat, J. Gaillardet, R. Freydier, Appl. Geochem. 24 (2009) 810.
[10] C.J. Park, Bull. Korean Chem. Soc. 23 (2002) 1541.
[11] S. Chandra, D.R. Lorey, D.R. Smith, Radiat. Res. 157 (2002) 700.
[12] M.C.B. Moraes, J.G.A. Brito Neto, C.L. do Lago, J. Anal. Atom. Spectrom. 16 (2001) 1259.
[13] G.L. Klunder, P.M. Grant, B.D. Andresen, R.E. Russo, Anal. Chem. 70 (2004) 1249.
[14] J.S. Becker, H.J. Dietze, Spectroscopy Europe 10 (4) (1998) 14–20 (references therein).
[15] B.A. Mamyrin, V.I. Karataev, D.V. Shmikk, V.A. Zagulin, Sov. Phys. JETP 37 (1973) 45.
[16] M. Joseph, N. Sivakumar, P. Manoravi, R. Balasubramanian, Rapid Commun. Mass Spectrom. 18 (2004) 231.
[17] P.V. Ramalingam, M.A.K. Iyer, R. Veerasamy, S.K. Gupta, L. Soosainathan, V. Rajan Babu, Proceeding of a Technical Committee meeting on 'Absorber materials, control rods and designs of shutdown systems for advanced liquid metal fast reactors' IAEA-TECDOC-884, PC International Atomic Energy Agency, Vienna, IAEA-TECDOC-884, 1996, pp. 60–67.
[18] D. Simeone, O. Hablot, V. Micalet, P. Bellon, Y. Serruys, J. Nucl. Mater. 246 (1997) 206.
[19] M. Joseph, P. Manoravi, Appl. Phys. A 76 (2003) 153.
[20] S. Becker, H.-J. Dietze, Int. J. Mass Spectrom. Ion Proc. 82 (1988) 287.
[21] L. Brewer, Principles of high temperature chemistry, vol. VI, in: Proc. Robert A. Welch Foundation, Conferences in Chemical Research, 1962, p. 47.
[22] O. Gebhardt, D. Gavillet, J. Nucl. Mater. 279 (2000) 368.
[23] X. Deschanels, D. Simeone, J.P. Bonal, J. Nucl. Mater. 265 (1999) 321.
[24] J.S. Becker, Inorganic Mass Spectrometry-Principles and Applications, John Wiley & Sons Ltd, England, 2007, p. 49.
[25] A.A. Sysoev, A.A. Sysoev, Eur. J. Mass Spectrom. 8 (2002) 213.
[26] C.P. Reddy, Internal communication, IGC/ROD/TSW/CPR/04 (2004).